SUBCONTRACT TITLE: SPUTTERED II-VI ALLOYS AND STRUCTURES FOR TANDEM PV

SUBCONTRACT NO: XAT-4-33624-06

QUARTERLY TECHNICAL STATUS REPORT FOR: Phase 1/Quarter 2

SUBMITTED TO: Martha Symko-Davies
National Renewable Energy Laboratory

PRINCIPAL INVESTIGATOR: A.D. Compaan
CO-INVESTIGATORS: V. G. Karpov and Robert Collins, Dept. of Physics and Astronomy
Dean Giolando, Department of Chemistry
University of Toledo,
2801 W Bancroft, Toledo, OH 43606

This progress report covers the second quarter of Phase 1 for the period March 9, 2004 through June 9, 2004 of the above referenced Phase IB High Performance PV contract. In this report we will give highlights on one activity within Task 1, the development of *in situ* real-time spectroscopic ellipsometry (RTSE) in our sputter deposition system, and two Task 5 activities: *ex situ* SE studies of the window-layer materials glass and SnO_2, and Raman and SEM characterization of chloride-treated CdMnTe.

Task 1: Sputtered top cell II-VI alloys--*RTSE development*

Real time spectroscopic ellipsometry (RTSE) based on the rotating-compensator principle has been implemented on the two-chamber sputtering system used for CdTe and related alloy deposition. The spectral range of the instrument is 0.75 to 6.5 eV, and full spectra in the ellipsometric angles (ψ, Δ) can be collected as an average over two optical cycles in a time as short as $(30.7\ \text{Hz})^{-1} = 32$ ms, where 30.7 Hz is the rotation frequency of the compensator. This instrument was purchased commercially, but is similar in design to an instrument first developed at Penn State University under the Thin Film Photovoltaics Partnership Program to study the growth of a-Si:H solar cells.[1] Figure 1 shows the time evolution of (ψ, Δ) at 6 out of the 706 spectral positions acquired during CdTe sputter deposition at 50 W target power and 18 mTorr Ar pressure using a native oxide covered (13.9 Å) crystalline Si wafer substrate, held at a nominal temperature of 200°C. This was the second RTSE experiment performed during CdTe deposition with the new instrument. The first deposition was performed on a rough thin film Mo-coated glass substrate; whereas for greater ease of analysis, the second deposition was performed using the c-Si wafer substrate due to its smoothness. Future experiments will use both superstrate and substrate solar cell configurations, and will also be performed during substrate rotation (rather than fixing the substrate as in the first experiments).

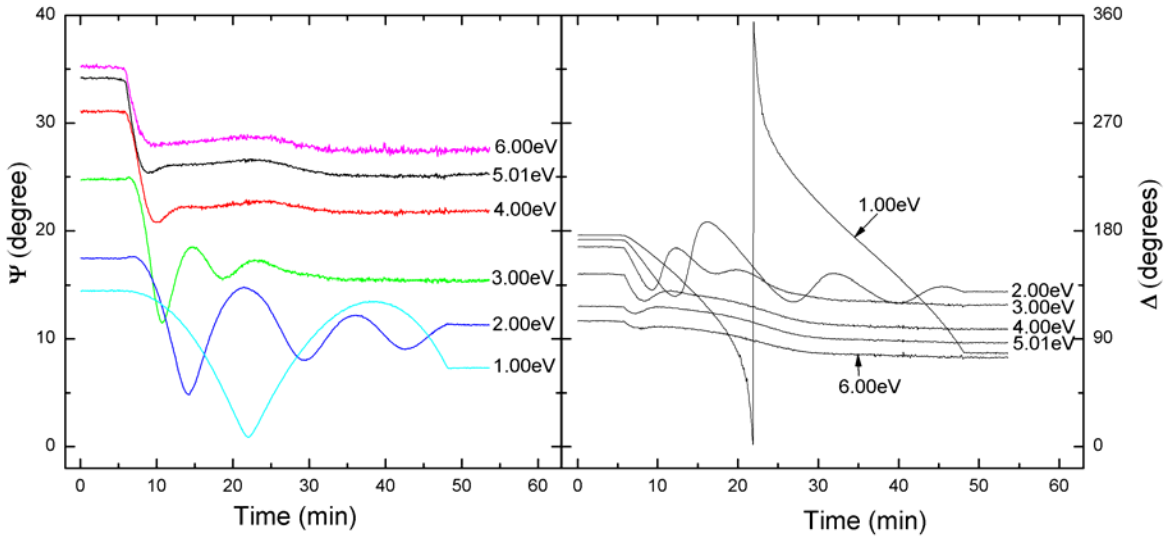

Fig. 1 Evolution of (ψ, Δ) at 6 selected photon energies from spectra acquired during CdTe sputter deposition on a native oxide covered crystalline Si wafer held at a nominal temperature of 200°C. The angle of incidence of the measurement was 65.61°.

Initial analysis of these spectra used specialized inversion/(least-squares regression) software developed at Penn State University under NREL support,[2] now used at University of Toledo. Commercially-available software is insufficient for extracting information from RTSE data for materials with complicated dielectric responses and extensive surface roughness development. Figure 2 shows the results of this analysis. The left side of Fig. 2 shows the time evolution of the microstructure, including the surface roughness layer thickness and the bulk layer thickness, as well as the quality of the fit σ_E averaged over energy and plotted vs. time (top). The right side of Fig. 2 shows the deduced dielectric function of the CdTe film, characteristic of the deposition temperature (nominal 200°C), along with room temperature reference data for single crystal CdTe.[3] At the top, another measure of the quality of the fit σ_t is given, which is averaged over time and plotted versus photon energy. In the best possible situation, the two measures of the quality of fit should be ~0.01 or less and show no variations versus time or photon energy.

The useful information that can be extracted from the left side of Fig. 2 includes the deposition rate and final film thickness, as well as the nucleation behavior and surface roughness evolution, the latter providing information on grain growth processes. The inset shows the initial few minutes of growth on a monolayer scale. In the pre-sputtering time before the shutter is open, ~1/3 monolayer (ML) of film material forms via gas phase diffusion around the shutter. When the shutter is opened any clustering associated with nucleation is at the level of a single ML, and once the bulk film is established, surface roughness develops immediately. The quality of fit degrades significantly as the roughness layer increases above 50 Å in thickness. It is likely that a more complicated multilayer or graded layer model for the surface roughness is needed in this thickness range. Future work will focus on improvements in the fit and corroborating the results by scanning probe microscopy.

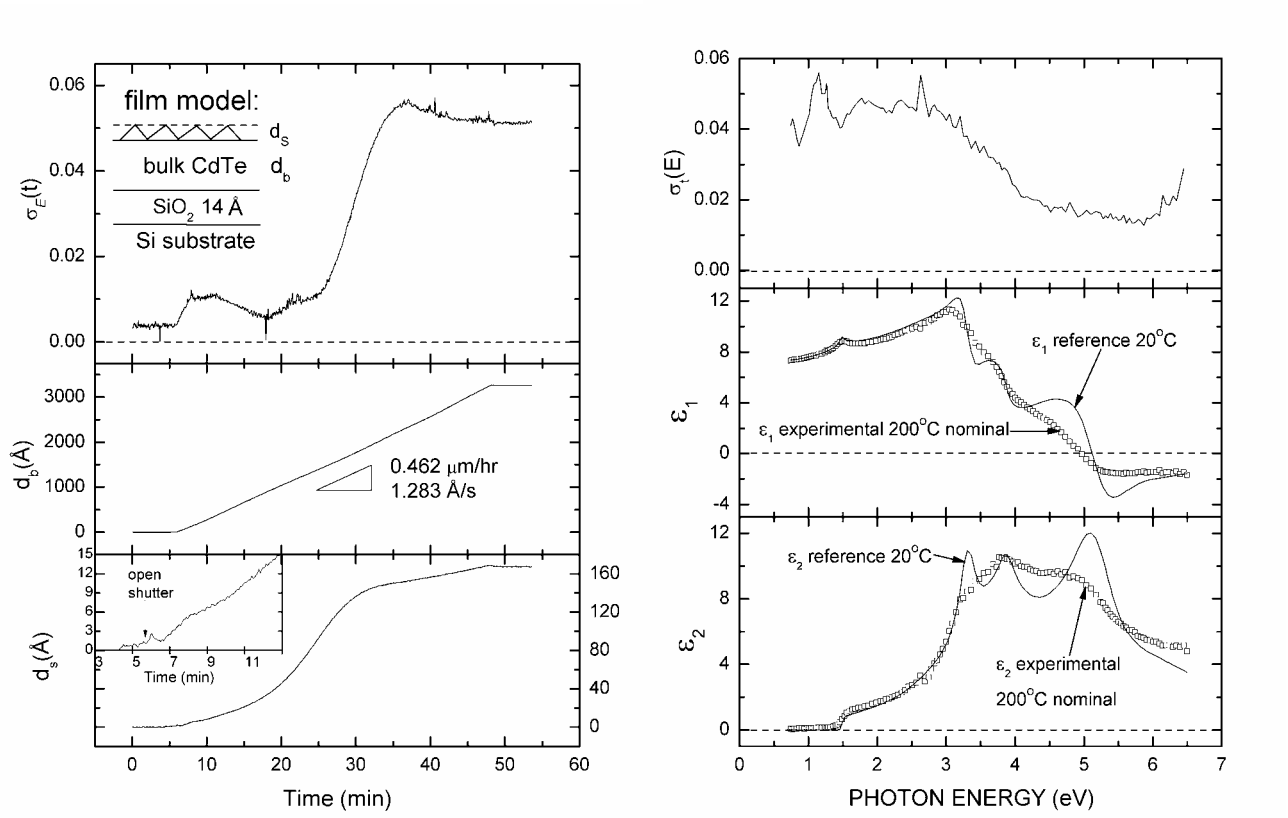

Fig. 2 (left) Evolution of the microstructure, including the surface roughness layer thickness d_s and the bulk thickness d_b, as well as the quality of the fit σ_E averaged over energy and plotted vs. time; (right) the deduced dielectric function of the 884Å CdTe film at the deposition temperature (nominal 200°C), reference data for single crystal CdTe at 20°C, as well as the quality of the fit σ_t averaged over time and plotted vs. energy.

The useful information that can be extracted from the right side of Fig. 2 is the optical properties of the growing film -- at the temperature of the deposition process. Measurements have also been made in real time as the film is cooled and at room temperature; however, for analysis of these spectra an improved model for the roughness layer is required, as noted at the end of the previous paragraph. Because the dielectric function of the CdTe film in Fig. 2 was extracted in an exact mathematical inversion process when the bulk and surface roughness thicknesses were 884 and 33 Å, respectively, the results here can be considered to be accurate. In support of this, the index of refraction below the band gap (which is given by $n = \sqrt{\varepsilon_1}$) is the same as that for the single crystal, which would be expected for a film of single-crystal density. It should be noted that the fit degrades below 4 eV, an effect attributed to that fact that during sputtering the substrate is heated by the deposition flux, and this alters its dielectric function. The effect could be taken into account in the future, once a successful parameterization of the T-dependence of the Si optical properties is established, however, this substrate is generally not of great interest, so this effort will be of low priority.

Perhaps of higher priority is to establish the nature of the critical points in the CdTe film optical properties. These can be seen in Fig. 2 (right) as being much broader than those in single crystal CdTe, due to the fine-grained nature of the polycrystalline film. The critical points that are evident in the film

spectra include the E_0 (fundamental gap), the E_1 and $E_1+\Delta_1$, and the $E_2(X)$ transitions. It is expected that the tabulated widths of these four critical points will provide key information on grain size. Ultimately the evolution of the critical point widths with thickness are sought since these will provide information along with the surface roughness evolution on grain coarsening vs. thickness. Finally in Fig. 2 it can be observed that the four critical points for the film are lower in energy than those in the single crystal. This is an effect of the nominal temperature difference, an effect that will be exploited in the future to deduce the true surface temperature of the film during sputtering, a notoriously difficult measurement to make for rotating substrate holders.

In a related direction, the substrate temperature has been calibrated using RTSE from a Si wafer mounted on the stationary substrate platform during heat/cool/heat cycles before deposition of the CdTe film on its surface, i.e., before the experiment of Fig. 2. In Fig. 3 data from two heating cycles and one cooling cycle and from two different critical point energies, ($E_0'+E_1$) and $E_2(X)$, are shown, i.e., six independent measurements in all. The energies were obtained by taking the second derivative of the dielectric function and fitting the results to expressions based on the parabolic band critical point approximation, along with the known room temperature values of the critical point energies and their functional dependence on temperature.[4] This is a standard procedure first developed by one of the investigators on this project.[5] A nominal temperature of 200°C is observed to correspond to a true temperature of 130°C. The standard deviation of the data from the linear fit is about 9°C. It should be kept in mind that during sputtering, substrate heating will occur so that the discrepancy may not be as dramatic. This heating will be assessed through measurements of the critical point energies of the growing CdTe film, as noted in the previous paragraph.

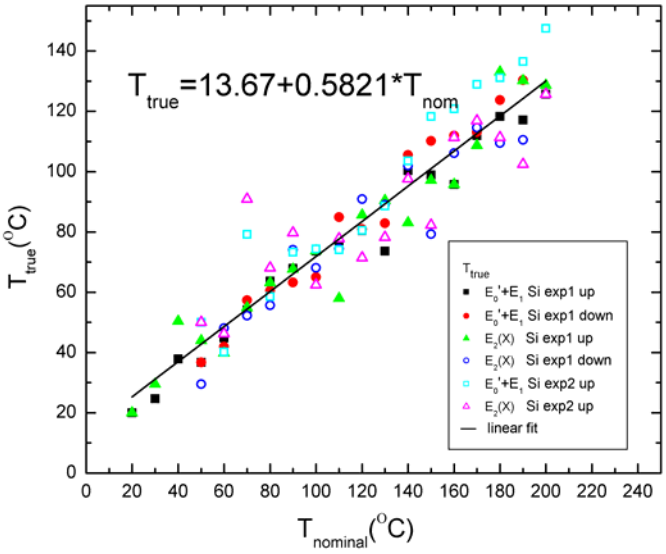

Fig. 3 Substrate temperature calibration for a c-Si wafer mounted onto the stationary substrate holder performed for an analysis of the $E_0'+E_1$ and $E_2(X)$ critical points.

Task 5 Characterization and stress studies

Ex situ spectroscopic ellipsometry

Ex situ spectroscopic ellipsometry studies were begun on glass/TCO structures (TEC-15 glass) used for superstrate solar cell fabrication at UT. Extremely accurate optical data for the glass and TCO are sought for careful accounting of optical losses in the solar cell. High accuracy requires careful procedures in an initial series of experiments to eliminate the incoherent multiple reflections of the light beam from the back surface of the glass (sun side in the case of the TCO measurement) in the SE measurement. First, to determine the optical properties of the glass, the sun side was measured for a glass/TCO structure in which the TCO film side was roughened to remove the film completely and then painted black to ensure no diffuse light from the rough interface returns to the detector. This led to a single air/glass interface for careful SE measurement of (n, k) for the glass from 0.75 to 6.5 eV. For the TCO film optical properties, the sun side (bare glass side) was roughened and painted black in order to eliminate from the optical problem the multiple incoherent back-reflections from this interface. Figure 4 shows the measurements in this case made before sun side treatments, then after the roughening, and finally after the roughening and painting. In summary, these results show that (i) the sun side treatment procedure used here somehow damaged the TCO surface and needs to be improved, (ii) the treatment procedure improves the visibility of the fringes, as would be expected from the removal of incoherent

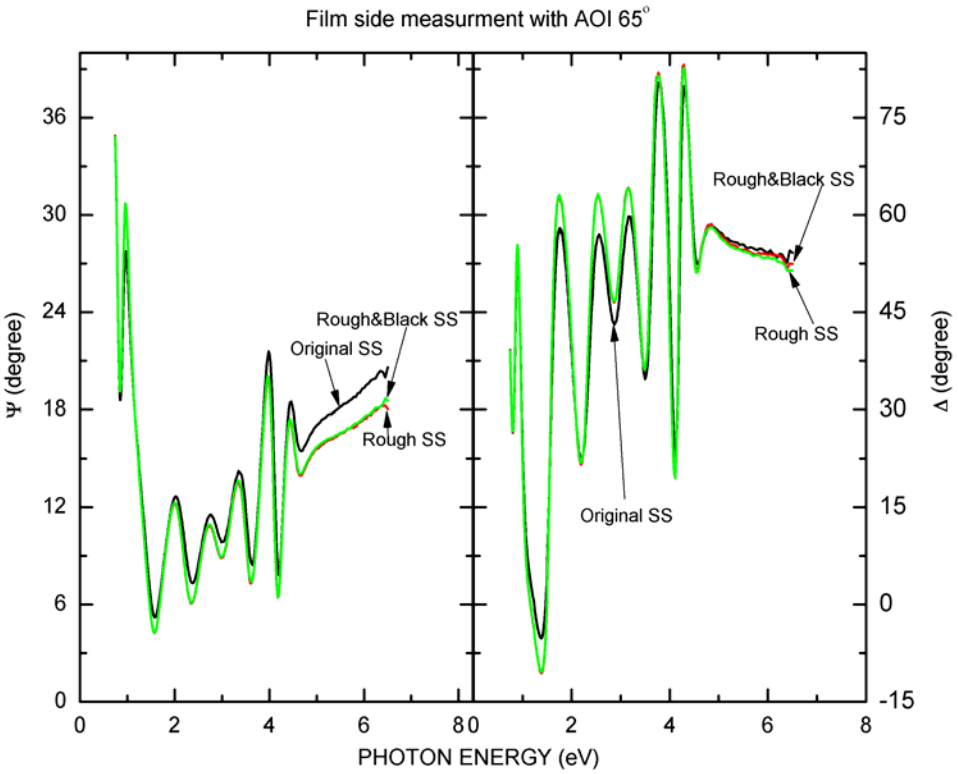

Fig. 4 Ex situ ellipsometric spectra collected at an angle of incidence of 65.00° for a TCO/glass structure measured at room temperature from the film side; the sun side is either measured (i) as received, (ii) after roughening to eliminate back-reflection, or (iii) after roughening and painting black.

light in the reflection process (thus, a partial success), and (iii) the black paint step is unnecessary. Finally, the visible range antireflection effect of the TCO is noted by the dampened fringes in ψ over the spectral range of 1.5 to 4 eV with a minimum near 3 eV. Future efforts will be made to better protect the TCO surface while the treatments are being done.

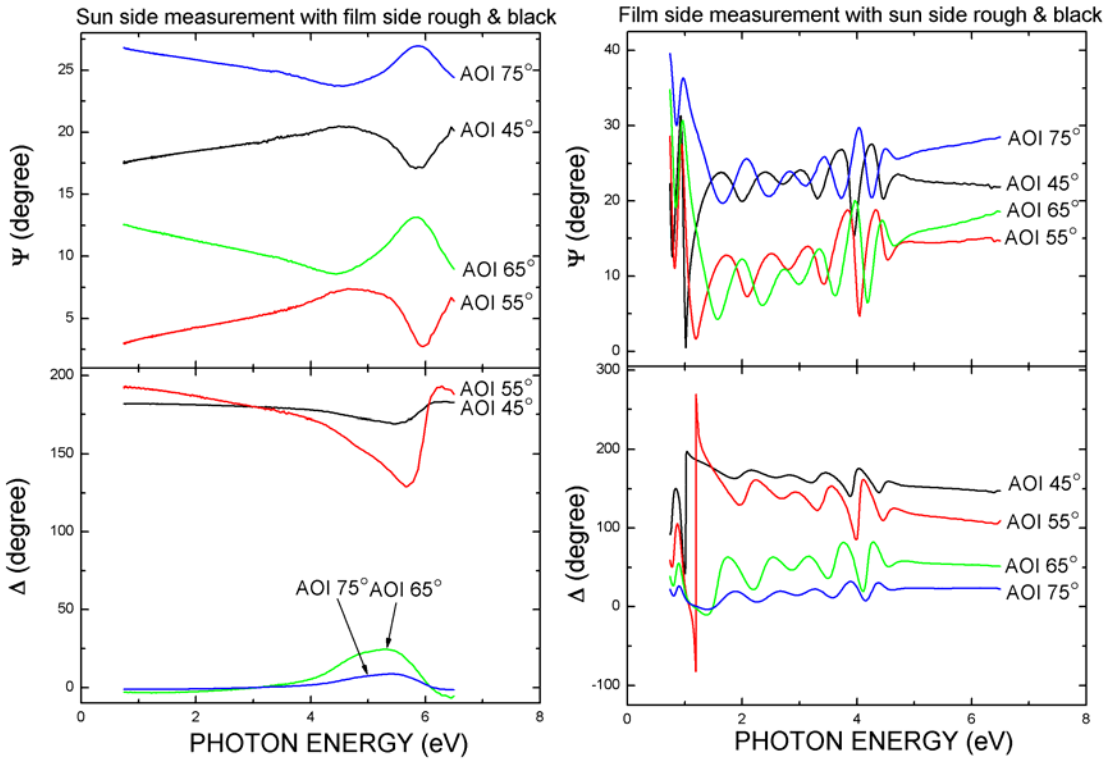

Fig. 5 Ellipsometric spectra for (left) a single ambient/glass interface and (right) a ambient/(TCO film)/glass structure. Incoherent back surface multiple reflections were avoided by roughening the back glass surface and painting it black.

Figure 5 shows examples of the measurements collected to extract optical properties and structure of the solar cell components. These data consist of (ψ, Δ) spectra collected at four angles of incidence: 45°, 55°, 65°, and 75° to be simultaneously fit to extract an expression for the index of refraction of the glass (at right), and the thickness and (*n*, *k*) spectra of the components of the TCO. This fitting is time consuming and will not be initiated until the problem noted in the previous paragraph is resolved.

Characterization of chloride-treated CdMnTe films

In the first quarter report, we reported on adopting a somewhat different approach to the post-deposition activation treatment, namely to shorten the time during which the film is exposed to high temperature and high chlorine partial pressures. According to the near-IR transmission results, the transmission edge of short-time annealed samples remained the same as before annealing, although the performance of cells fabricated using this post-deposition chloride treatment was improved over that of

cells with no treatment. Still the currents and voltages were low. During the second quarter, we used optical techniques including Raman spectroscopy as well as scanning electron microscopy (SEM) to investigate characteristics of chloride-treated CdMnTe films.

The thickness of the CdMnTe samples is about 1μm, the content of Mn is about 5% (E_g=1.63eV at RT). The annealing process includes preheating at high temperature (either 400 °C or 520 °C) for 10 min in a reducing gas atmosphere, 2% H_2 in Ar, and annealing in the mixed vapors of $CdCl_2$ and $MnCl_2$ in dry air at lower temperature (360 °C or 380 °C) for either short (2 min) or long times (30 min). Raman scattering was carried out at room temperature (RT) with 30 mW of 514 nm Ar ion laser excitation. Fig. 6(a) displays the Raman spectra of as-deposited samples. The TO-phonon and LO-phonon modes of the CdTe sample are observed at 146±4 cm^{-1} and 170±4 cm^{-1}, respectively. For CdMnTe samples, the peaks at 141 cm^{-1} and 164 cm^{-1} are correspond to the CdTe-like TO and LO-phonons. Fig. 6(b) shows the Raman spectra of samples after various chloride treatments.

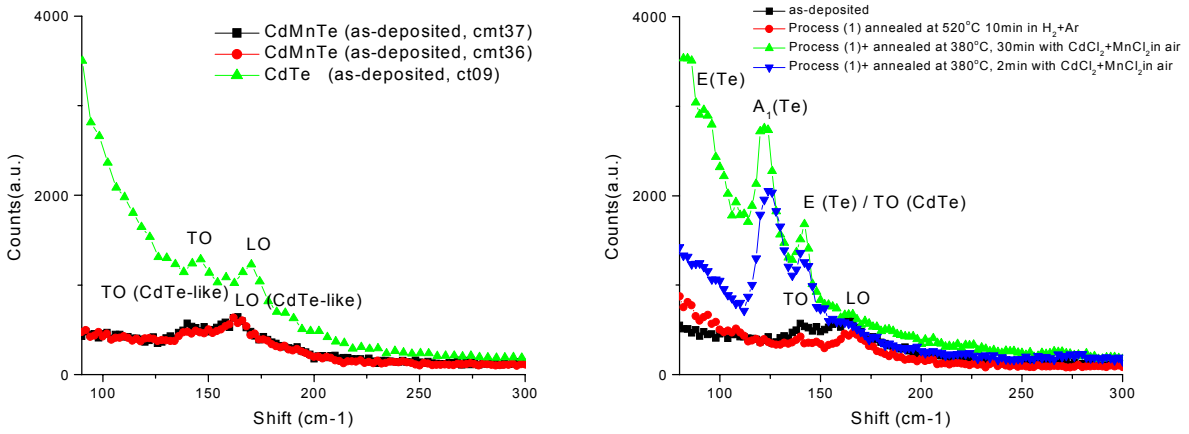

(a) (b)

Fig. 6 Raman spectra of as-deposited (a) and chloride treated (b) $Cd_{1-x}Mn_xTe$ samples

After 520 °C, 10 min annealing in the H_2 + Ar gas, the Raman spectrum shows little difference from that of the as-deposited sample. But after 380 °C annealing in mixed chloride ambient, additional peaks (124 cm^{-1} and 142 cm^{-1}) occur in the spectra. In references 6 and 7, these peaks are related to Te precipitates in CdTe crystals, the peak around at 124 cm^{-1} is due to the phonon with A_1 symmetry, the 92 cm^{-1} and 142 cm^{-1} peaks correspond to phonons with E symmetry.

Similar Raman spectra were observed on samples we treated with NH_4Cl vapors for which the preheating temperature was about 400 °C. The spectrum of the sample annealed at 400 °C for 10 min in the H_2 + Ar gas is similar to that of the as-deposited sample. The sample annealed at 370 °C for 15 min with NH_4Cl also shows Te-related phonon peaks, similar to the sample pre-annealed at 520 °C followed by low temperature annealing in the mixed chloride vapors.

Fig. 7 displays SEM images of samples treated at these conditions. As-deposited samples showed mirror-like surfaces, with very smooth surface morphology. However, the mirror-like surface turned rough after Cl treatment. It is noted that long time or high temperature mixed chloride vapor treatment results in a spotted surface and makes the film fragile (easily scratched and delaminated).

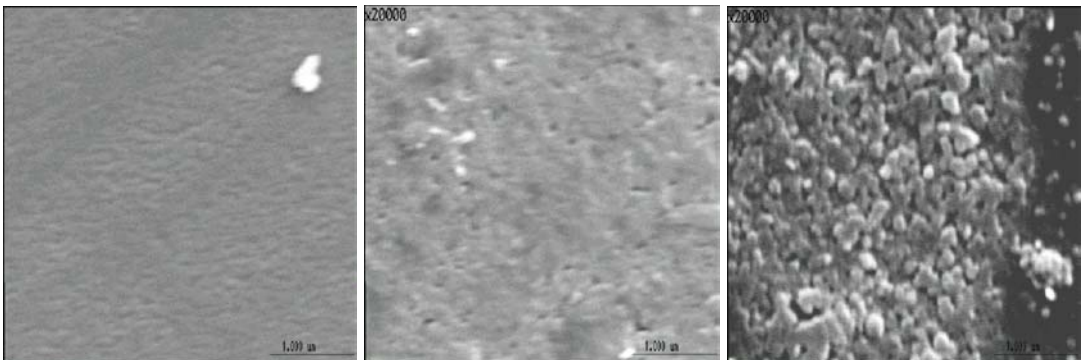

(a) (b) (c)

Fig. 7 SEM images of CdMnTe at different treatment conditions, (a) as-deposited sample, (b) preheated (520 °C) + 2 min 380 °C mixed chloride treatment, (c) preheated (400 °C) + 15 min 380 °C mixed chloride treatment.

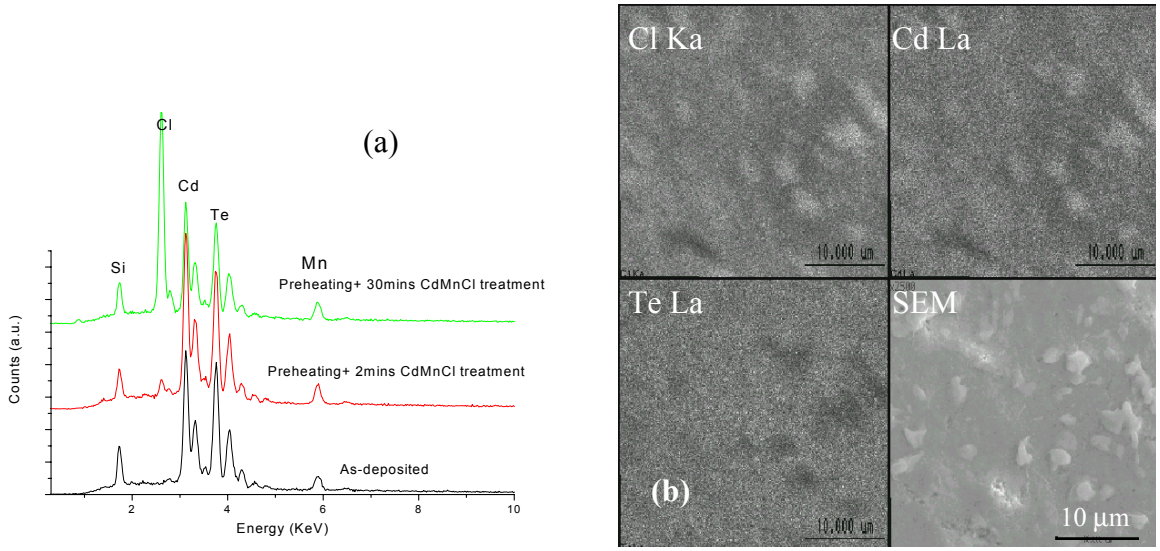

Fig. 8. (a) EDS of as-deposited and Cl treated samples. (b) X-ray mapping and SEM images of 30 min mixed chloride treated CdMnTe sample.

For mixed-Cl-treated samples, we observed the elemental Te peak in the Raman spectra and found textured structures on the surface. To further investigate the elemental composition of the surface structures, we used EDS and x-ray mapping. Fig. 8(a) shows the energy dispersive x-ray spectra, EDS, of as-deposited and mixed-Cl-treated samples. The main peaks indicate the films are mainly composed of Cd, Te and Mn, and their intensity does not vary drastically from each other. However, an intense Cl peak is observed in the 30 min mixed-Cl-treated sample. Fig. 8(b) shows x-ray mapping and SEM images of the 30 min mixed-Cl-treated sample. Cd-rich and Cl-rich spots were observed in Cd and Cl x-ray map, respectively, it suggests the spots are mainly composed of Cd and Cl. These spots may contain oxygen as well since oxygen peak was not detected and Cl-treatment was carried out in dry air.

We found Te-related peaks (124 cm^{-1}, 142 cm^{-1}) in the Raman spectra, these Raman shifts correspond to Te precipitates (see Ref.6 (120 cm^{-1}) and Ref.7 (127 cm^{-1})). If TeO_2 exists on the top layer, we should observe another peak at 648 cm^{-1}. Indeed, we found this peak on 30 min-treated sample, but could not find on 2 min-treated sample. According to EDS data, there is a Cl peak in our sample, and X-ray mapping on 30 min-treated sample indicated some spots composed of Cd and Cl

content, it is reasonable to consider $CdCl_2$ sublimed on the film due to 1mm distance between sample and $CdCl_2$ source, But after DI water rinsing, EDS shows the ratio of Te/Cd is much high than that of as-deposited sample, this is consistent with appearance of Te-releated peaks in Raman spectra. The appearance of Cl in the EDS data indicates the presence of some Cl-related compounds, such as $TeCl_2O$ or $TeCl_4$. Niles, et al[8] investigated the chemical reaction of wet Cl treatment of CdTe films (400 ^oC, 30 min) by x-ray photoelectron spectroscopy, they proposed that CdO, TeO_2, $TeCl_2O$ are building blocks for the surface Cl residue. Te-related peaks (124 cm^{-1}, 142 cm^{-1}) can be observed in the Raman spectra, that means the surface is mostly compose of elemental Te (short time 2 min annealing) or TeO_2 (long time 30 min annealing).

Thus, we observed Te-related peaks in Raman spectra, probably due to Te precipitates or TeO_2 components. EDS and X-ray mapping indicated $CdCl_2$ had sublimed onto the surface. Compared with Cl-treated CdTe films, we do not observe Te-related peaks in Raman spectra, CdMnTe films show some Te enrichment after Cl treatment, this demonstrates that Cl treatment is complex in alloy materials.

References

1. J. Lee, P. I. Rovira, I. An, and R. W. Collins, *Review of Scientific Instruments* **69**, 1800 (1998).
2. I. An, Y. M. Li, H. V. Nguyen, C. R. Wronski, and R. W. Collins, *Applied Physics Letters* **59**, 2543 (1991).
3. E. D. Palik (ed.), *Handbook of Optical Constants of Solids* (Academic, Orlando, 1985), p. 409.
4. P. Lautenschlager, M. Garriga, L. Viña, and M. Cardona, *Phys. Rev. B* **36**, 4821 (1987).
5. M. Wakagi, B. Hong, H.V. Nguyen, R.W. Collins, W. Drawl, and R. Messier, *Journal of Vacuum Science and Technology A* **13**, 1917 (1995).
6. S.H.Shin, J.Bajaj,L.A.Moudy and D.T.Cheung, *Appl.Phys.Lett.* **43**, 68 (1983).
7. P.M.Amirtharaj, and Fred H. Pollak, *Appl. Phys. Lett.* **45**, 789 (1984).
8. D.W.Niles, D. Waters, D. Rose, *App.Surf. Sci.* **136**, 221 (1998).